



Contribution of permanent stations GPS data to estimate the water vapor content over Algeria

Hassen Abdellaoui¹ · Naima Zaourar¹ · Salem Kahlouche²

Received: 15 March 2018 / Accepted: 8 January 2019 / Published online: 25 January 2019
© Saudi Society for Geosciences 2019

Abstract

In the last decade, important studies have demonstrated that GPS can be also used as an efficient tool for measuring the integrated water vapor (IWV) in the atmosphere which is a useful quantity for climatological and weather forecasting applications. This study presents the first results obtained by using the time series GPS stations of six local stations belonging to the continuously operating Algerian network, and 13 stations of the IGS (International GNSS Service) for the estimation of the value of the IWV locally. In this paper, tropospheric parameters are obtained from double difference processing of GPS observations, collected from 2008 to 2015, using the Bernese 5.2 software. For the validation of GPS IWV values, three approaches are used. In the first, the GPS IWV are compared with the corresponding ERA-Interim values derived from interpolations in time and space. The results show a good agreement with correlation coefficients exceeding 85% and an RMS (root mean square) between 2.22 and 5.53 kg m⁻². In the second approach, we compare GPS IWV and radiosondes over two stations, where the results showed an acceptable concordance and equivalent to those of the first approach. In the third approach, the GPS ZWD (zenith wet delay), roughly IWV, values are compared with the daily rainfall data provided by the Algerian Meteorological Office. The results show that the temporal variation of ZWD and the high rainfall collected by rain gauges (not far from those of GPS) present a perfect coincidence over the surrounding observed peaks. Finally, the analysis of the annual time cycle of ZWD and precipitation carried out on the data of geographically and climatically different GPS stations shows that these two parameters depend on the latitude of the site. The first experimental results of this study further strengthen the strong potential of GPS in meteorological applications.

Keywords GNSS/GPS · Integrated water vapor · ERA-Interim · Precipitations

Introduction

Water vapor is considered the most parameter of major constituents in atmospheric process acting as the principal resource for precipitation in all weather system.

Like the areas on the Mediterranean's borders, some Algeria regions often undergo specific meteorological episodes characterized by intense rainfall lasting from 2 to 3 days with accumulations three times higher than monthly averages. These areas are also affected by flash floods in autumn, strong winds and swells in winter, and heat waves and drought in summer. It is difficult to predict these exceptional events that cause human and material damage. One way to improve predictions would be to use estimates of water vapor quantity in the atmosphere by GNSS. Indeed, the GNSS is one of the only instruments of measurement of functional water vapor even in the presence of clouds in the atmosphere.

The continuous improvement of data processes, precision of GNSS products keeps growing, primes that GNSS-integrated tropospheric water vapor contents are valued references for the evaluation of atmospheric models. The practically 30 years GNSS network measurements offer a novel and accurate dataset leading to a better estimate integrated water vapor.

✉ Hassen Abdellaoui
abdhasen@hotmail.fr

Naima Zaourar
nzaourar@usthb.dz

Salem Kahlouche
kahlouche@asal.dz

¹ Geophysics Department-FSTGAT, University of Sciences and Technology Houari Boumediene (USTHB), BP 32 El Alia, 16111 Algiers, Algeria

² Department of Space Geodesy, Center for Space Techniques, 31200 Arzew, Algeria

Many studies (Bevis et al. 1992; Baltink et al. 2002; Guerova 2003, Guerova et al. 2016; Boutiouta and Lahcene 2013; Namaoui et al. 2017) have shown that global positioning system (GPS) is an efficient tool for sensing the integrated water vapor (IWV) content in the atmosphere.

During its propagation through the atmosphere, the GPS signal is affected by atmospheric constituents, including water vapor, considered the most variable of the major constituents. Precipitable water or IWV is defined as the total atmospheric water vapor enclosed in a vertical column from the Earth's surface to the top of the atmosphere.

GPS techniques and means are increasingly used to determine IWV from GPS signal delays (Bevis et al. 1992). The delay of the radio signals transmitted by GPS satellites is closely linked to the water vapor content along the atmospheric signal path. To date, ground-based GPS meteorology has provided high-frequency (~5 min) and low-cost IWV values with 1–2 mm accuracy relative to radiosondes and radiometer sunder all weather (Rocken et al. 1993; Wolfe and Gutman 2000; Haase et al., 2003; Li et al., 2003). Bock et al. (2007a, b) have inter compared IWV measurements from observing techniques such as ground-based GPS, radiosondes, AERONET (AERosol ROBotic NETwork) sun photometers, and SSM/I (Special Sensor Microwave Imager), as well as reanalyzes from European Centre for Medium-Range Weather Forecasts (ERA-40) and National Center for Environmental Prediction (NCEP2) over Africa. They presented that good agreement in IWV was found between observational techniques and reasonable agreement was found between the observational datasets and ERA-40 (NCEP2) reanalysis. Namaoui et al. (2017) have shown a good agreement between GPS and radiosondes over Algeria. In that, ground-based GPS meteorology is capable to offer high accuracy IWV estimates which are useful in the studies of weather and climate over Africa. The high spatial and temporal resolutions of GPS IWV measurements are exploited to examine surface moisture versus IWV at definite locations, different elevations, and various sky conditions.

The main purpose of this paper is to use the time series of six (06) local stations belonging to the continuously operating Algerian network, and thirteen (13) stations of the IGS (International GNSS Service) to estimate locally the value of IWV in the atmosphere. We are interested in this study to assess the degree of correlation and reliability of IWV values calculated by GPS data, IWV values derived from the European Center for Medium-Range Weather Forecasts (ECMWF) (Böhm et al. 2006; Berrisford et al. 2009), and the IWV obtained from radiosonde sites (Namaoui et al. 2017).

We looked closely also at some rainfall peaks recorded by meteorological stations in some locations during the year. Finally, we examine the zenith wet delay (ZWD), in other

words, indirectly water vapor saturation and analyze the correlation between peaks of ZWD and rainfall.

To carry out this work, we look at the six GPS stations (DZAL, DZOR, DZCO, BECH, and TIND) closest to the core of precipitation, which were almost collocated with rain gauges distant of less than 5 km. GPS measurements have been collected from 2008 to 2015 for DZAL, DZOR, and DZCO stations and from 2012 to 2015 for BECH and TIND stations.

In “GPS processing techniques” section, we present a summary of GPS processing method and analysis techniques. In “Dataset and data processing” section, we describe in the first part the selected GNSS network of ground-based GPS receivers and the processing of the GPS data. In the second part, we present the results of the analysis of the GPS IWV and radiosonde processing data. Finally, we discuss the behavior and reliability of GPS IWV values at the time of precipitations classified as peaks by the National Meteorological Office and its look during the annual cycle. Conclusion is given in “Conclusion” section.

GPS processing techniques

GPS network and processing

In terms of GPS processing, there are two main accepted methods: double difference (DD) and precise point positioning (PPP) (Ge et al. 2008). The main difference between DD and PPP processing strategies is that PPP is a station-wise solution whereas DD is a network approach. In PPP, if there is a problem with one station, it will not affect the solutions of other nearby stations. Also, as the processing is station specific, the load of processing can be run in parallel on a number of CPU's or even on parallel servers. In this way, the actual GPS processing part of PPP is much quicker than DD. However, for PPP to be effective, very precise satellite clock values have to be available. In DD processing, baselines between stations in the network are formed; consequently, the clock errors in the phase GPS equations can be eliminated. There are however negatives to DD processing.

Firstly, the processing is much slower, as baselines as well as the receiver-satellite distances have to be estimated. In addition, if there is a problem with one GPS station, this error will be introduced to the other stations, which it is connected to by way of the baselines (Jones 2010).

In this study, the DD strategy was used for the GPS data processing using the Bernese 5.2 processing software developed by the Institute of Astronomy of the University of Bern (AIUB). A daily estimate of coordinates for all sites is produced and has a 30-s time resolution. All GPS sites use choking antennas. The antenna mounts were concrete pillars fixed on the rooftops of buildings.

Six (06) local GNSS stations are used with thirteen (13) IGS stations (ISTA, DRAG, NKLK, SOFI, MAT1, MATE, MBAR, MEDI, TLSE, VILL, SFER, RABT, and MAS1). The raw data in the RINEX (Receiver Independent Exchange) format of the local and IGS dual-frequency stations are processed using the precise ephemeris and satellite clock corrections published by the IGS.

The a priori model corresponds to the dry component of the VMF (Vienna Mapping Function) explained in (Boehm et al. 2006). The pressure, temperature, and humidity parameters are derived from the atmospheric model of the European Center for Medium-Range Weather Forecasts (ECMWF). As recommended, site-specific tropospheric parameters are estimated using the wet component of the VMF1 mapping function. The time resolution used during the analysis is 2 h. A relatively low mask of 5° is used to decorrelate the troposphere estimates and the heights of the stations. The available tropospheric delays of the used IGS stations were introduced during the analysis (Dach et al. 2007). As a result, the troposphere solutions and the stations coordinates are stored in the so-called SINEX (Solution INdependent Exchange) tropospheric files.

ZTD and ZHD derived from GPS time series

For a decade, GPS observations have shown their ability to estimate the zenith tropospheric delay (ZTD). This total delay can be divided into the hydrostatic part defined as zenithal hydrostatic delay (ZHD) and wet part named zenithal wet delay (ZWD). Following Bevis et al. (1992), ZWD is closely linked to the water vapor in the atmosphere and can be transformed into IWV using a simple scale factor Π .

This factor is usually estimated as a function of the surface temperature by empirical equation derived from regional radiosonde observations (Bevis et al. 1992). Thus, GPS dense networks may provide vertically integrated tropospheric water vapor observations.

For further investigations, we examine data set recorded from a GPS network during 8 years from 2008 to 2015. The aim in this part is to describe humidity field locally in Algeria during rainfall episode.

The common analysis procedure is described in several publications (e.g., Bevis et al. 1992, 1994; Bock and Doerflinger 2001; Roeckner et al. 2003; Wang and Zhang 2009). Thus, we give only a brief overview here.

The tropospheric delay estimate is expressed as ZTD, which is decomposed into the zenith hydrostatic delay (ZHD) and the ZWD as is shown in the following relation:

$$ZTD = ZHD + ZWD \tag{1}$$

The ZTD yields the water vapor information.

To hydrostatic equilibrium, ZHD can be expressed as a function of surface pressure P_s , measured at GPS antenna.

Following Heise et al. (2009), the ZHD is expressed as:

$$ZHD = (2.2768 \pm 0.0005)P_s/f(\varphi, H) \tag{2}$$

Where ZHD is in mm and P_s is the surface pressure (in millibars).

and

$$f(\varphi, H) = 1 - 0.0026 \cos(2\varphi) - 0.00028H \tag{3}$$

The Relation 3 describes the dependence of gravity acceleration from latitude φ and surface height H (in Km) over the ellipsoid.

The ZWD estimates were then obtained by subtracting the ZHD from the ZTD data (Formula 1).

The relation between IWV and ZWD is given by the formula

$$IWV = ZWD \cdot \Pi \tag{4}$$

The factor Π depends on the water vapor-weighted atmospheric mean temperature T_m (Heise et al. 2009) as following:

$$\Pi^{-1} = 10^{-6} \rho H_2O R_v \left(\frac{C_2}{T_m} + C_2 \right) \tag{5}$$

Where:

R_v is the explicit gas for water vapor (461.45 J/kg/K), ρH_2O is the water density (1000 kg/m³). The two constants are determined by (Bevis et al. 1994):

$$C_1 = (3.739 \pm 0.012) 10^5 k^2 h P_a^{-1} \text{ and } C_2 = (2.21 \pm 2.2) Kh P_a^{-1}$$

The weighted mean temperature T_m of the atmosphere can be expressed as:

$$T_m = \frac{\int \frac{P_v}{T} dz}{\int \frac{P_v}{T^2} dz} \approx \frac{\sum_{i=1}^N \frac{P_i}{T_i}}{\sum_{i=1}^N \frac{P_i}{T_i^2}} \tag{6}$$

Where P_v is the partial pressure of water vapor, T the absolute temperature, and z the vertical coordinate.

T_m can be estimated from ECMWF weather forecasting models using the linear relation to air temperature at the ground surface T_s (Bevis et al. 1992):

$$T_m \approx 70.2 + 0.72 T_s \tag{7}$$

Estimation of the IWV at the station

The GPS signal delay in the atmosphere is established using the estimated delay introduced by the atmospheric water vapor during the GPS signal propagation.

We compare the values of the IWV derived from the ECMWF models to those obtained by the GPS time series during the year 2014 (the most complete year in recording data for Algerian stations). The IWV values of the ECMWF were extracted from the ERA-Interim (Berrisford et al. 2009) analysis archives throughout 2014. These values are structured in a reduced Gaussian grid with a time resolution of 6 h (at 0:00 h, 6: 00 h, 12:00 h, and 18:00 h) and a spatial resolution of $0.75^\circ \times 0.75^\circ$ (Dee et al. 2011). The downloaded data were in the NASA CDF format. The IWV of the node of the ECMWF grid closest to the GPS station is extracted for each station without considering the terrain topography.

First, we found that GPS IWV data are not directly comparable with IWV data from ERA-Interim due to the disparity between the geographical areas covered by the two data sources and the altitude difference relative to the sea level of the six stations.

To fix this, it is necessary to horizontally and vertically interpolate the IWV of the ERA-Interim at the position of the GPS station.

The horizontal interpolation of the IWV data of the ERA-Interim used at a station is performed by a weighted linear interpolation of the four corners of the grid surrounding the station. For the vertical interpolation, the parameters of temperature and specific humidity are structured vertically in 60 pressure levels, which divide the atmosphere. In this case, pressure $P = 1$ corresponds to stratosphere higher than about 65 km in height and $P = 60$ corresponds to the surface of the soil at the mean sea level (Abraha et al. 2017).

Integrating the geoid height derived from geopotential model EGM96 allows the conversion of the ellipsoidal height to the orthometric height with respect to mean sea level. IWV can be achieved using the specific humidity transferred with respect to the variation of the 60 full levels of pressure wherein the discrete case can be described by:

$$IWV_{ECMWF} = \frac{1}{g_0} \sum_{i=1}^{60} q(i) \Delta p(i) \quad (8)$$

$$\Delta p(i) = \Delta p(i + 1) - p(i) \quad (9)$$

Where g_0 is the acceleration of gravity at mean sea level, $q(i)$ is the specific humidity of the air at level i , $p(i)$ the atmospheric pressure at level i .

Spatial and temporal distribution of the water vapor in the atmosphere

Tropospheric delay and integrated water vapor (IWV) derived from the ECMWF ERA-Interim are extensively used in many atmospheric applications. Several studies have shown that the spatial and temporal IWV-derived differences between GPS IWV and ERA-Interim IWV are a function of topographic properties and climate changes. Note that the errors in GPS IWV are due to estimation of the ZTD and particularly when calculating ZHD from surface pressure interpolated and the conversion from ZWD to IWV (Hagemann et al. 2003), which is the case in this study.

Dataset and data processing

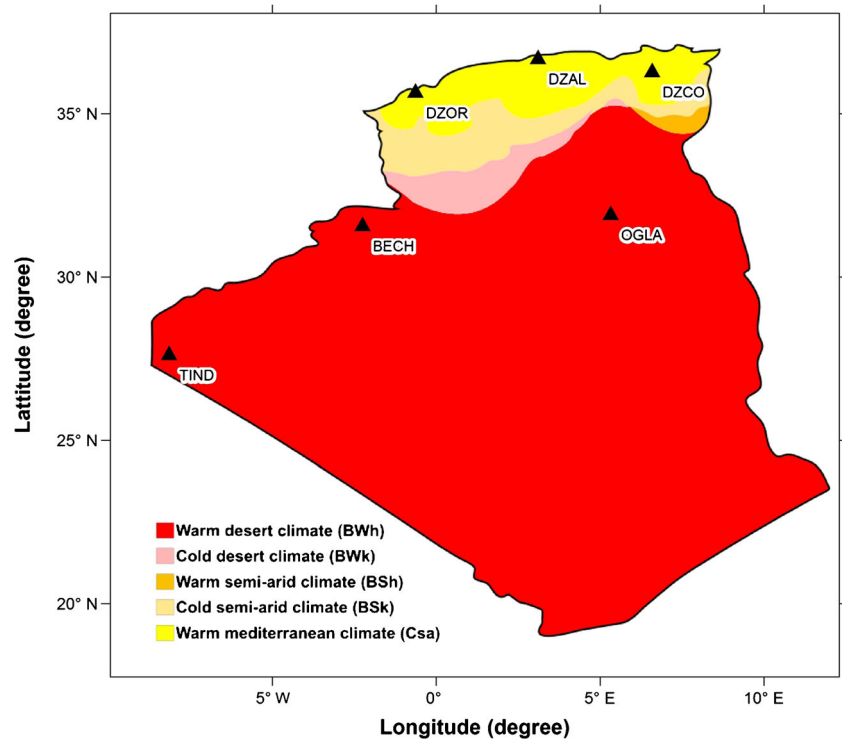
Climate and distribution of GNSS stations and radiosonde observations

Algeria is located between latitude 19° to 37° N and longitude 9° W to 12° E in Northern Africa. The area of the country is the largest in Africa, with $2,381,741 \text{ km}^2$. The relief of Algeria consists of three main sets: the Tell in the north, the highlands and the Saharan Atlas in the center, and the Sahara in the south which alone represents 84% of the territory.

The north is crossed from west to east by a double mountain barrier namely Tell Atlas and Saharan Atlas. The ground is covered with many forests in the center, vast plains in the east, and the Sahara. Figure 1 shows the localization of Algerian network and the Köppen classification of the climate and weather in Algeria (Chinowsky et al. 2013). As illustrated, the northern part has a warm Mediterranean climate (Köppen climate classification Csa), whereas the rest of the country has mainly a warm desert climate (Köppen climate classification BWh).

However, between these two major types of climates exist transition climates, including the cold semi-arid climate (Köppen climate classification BSk), which corresponds to a Mediterranean climate with a drought no longer limited solely to the summer season but good part of the year but also a Mediterranean climate with mountain influences, a little more continental. Nevertheless, Algeria is a subtropical country where the dominant climate is hot and dry. The Algerian Tell coastal part is characterized by an abundant rainfall, fluctuating from 400 to 670 mm annually. We note significant increase precipitations from west to east. In the northeastern part of Algeria, the amount of precipitation can reach up to 1000 mm in some years, while inland, the precipitations are much less abundant. During the summer, the prevailing winds are direction east and northeasterly and heading toward westerly and northerly in winter. These direction changes are accompanied by a substantial increase in precipitation from

Fig. 1 Algerian permanent GNSS network, northern stations (wet and costal climate): DZOR, DZAL, and DZCO and southern stations (dry climate, subtropical desert): TIND, BECH, and OGLA



September to December, a diminution in the late winter and spring months. The summer period is marked by an almost total absence of rainfall (Fig. 2).

The GNSS network in Algeria is currently composed of six operational stations. Three are located to the north and three to the south (Fig. 1). In its final version, the GNSS Algeria project aims to extend this network to more than 200 stations to

cover the whole country. Table 1 gives the geographic coordinates and height of the GNSS stations used in this study.

The three stations (DZAL, DZOR, and DZCO) located in the northern cities have a hot Mediterranean with dry-summer subtropical climate (Köppen-Geiger classification: Csa) that is mild with moderate seasonality. Summers are dry and hot due to the domination of subtropical high pressure systems while

Fig. 2 Average annual precipitation in Algeria

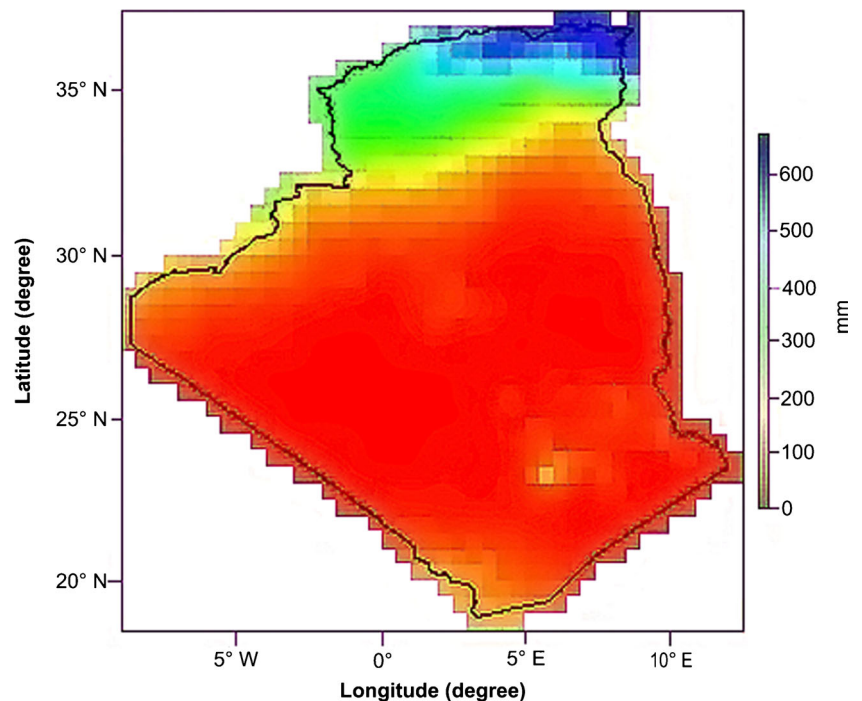


Table 1 Geographic coordinates and elevation of the six GPS stations used in this study

Station	Code	Latitude	Longitude	Height (m)
Algiers	DZAL	36° 44' N	3° 06' E	25.89
Oran	DZOR	35° 41' N	0° 37' W	134.25
Constantine	DZCO	36° 19' N	6° 35' E	547.58
Bechar	BECH	31° 37' N	2° 14' W	816.68
Ouargla	OGLA	31° 37' N	5° 19' E	146.54
Tindouf	TIND	27° 40' N	8° 9' W	411.90

winters experience moderate temperatures and changeable, rainy weather due to the polar front. These climates typically are present on the western parts of continents at latitudes among 30 and 45°. In the warmest month, the Mediterranean climate is distinguished by average temperatures exceeding 22 °C. In the coldest month, average temperatures oscillate between 18° and – 3 °C and at least 4 months display temperatures above 10 °C.

Seasonality is moderate (Köppen-Geiger classification: Csa). The last three stations (BECH, OGLA, and TIND) located in the southern cities have subtropical desert with low-latitude arid hot climate (Köppen-Geiger classification: Bwh).

For the radiosondes and for reasons of data availability for the same period (GPS and radiosondes) over a long period of time and in order to study two different climates, we were interested in two stations Algiers (WMO code 60390) located

in the north with Mediterranean climate and Bechar (WMO code 60571) located in the south with subtropical desert (see Fig. 3 and Table 3). The observations processed are those recorded during the years 2012, 2014, and 2015 and are downloaded from the University of Wyoming website (<http://weather.uwyo.edu/upperair/sounding.html>). All corrections due to the distance between GNSS stations and meteorological sites (less than 10 km), difference in altitude, surface temperature, and pressure were taken into account (Vey et al. 2009).

$$P_{GPS} = P \cdot e^{-g\Delta H/(R_d T)}$$

With:

P_{GPS} : Pressure at GPS antenna height (hPa)

$R_d = 287.053 [Jkg^{-1}K^{-1}]$ is the gas constant for dry air

P: the pressure at the height of the pressure sensor (hPa)

ΔH : $H_{GPS} - H_s$ the height difference (m)

T: mean temperature of the layer between meteorological sensor and GPS antenna (K°)

Data processing

A Matlab script has been developed for the conversion of the ZTD content to IWV. Figure 4 shows the ZTD (blue curve)

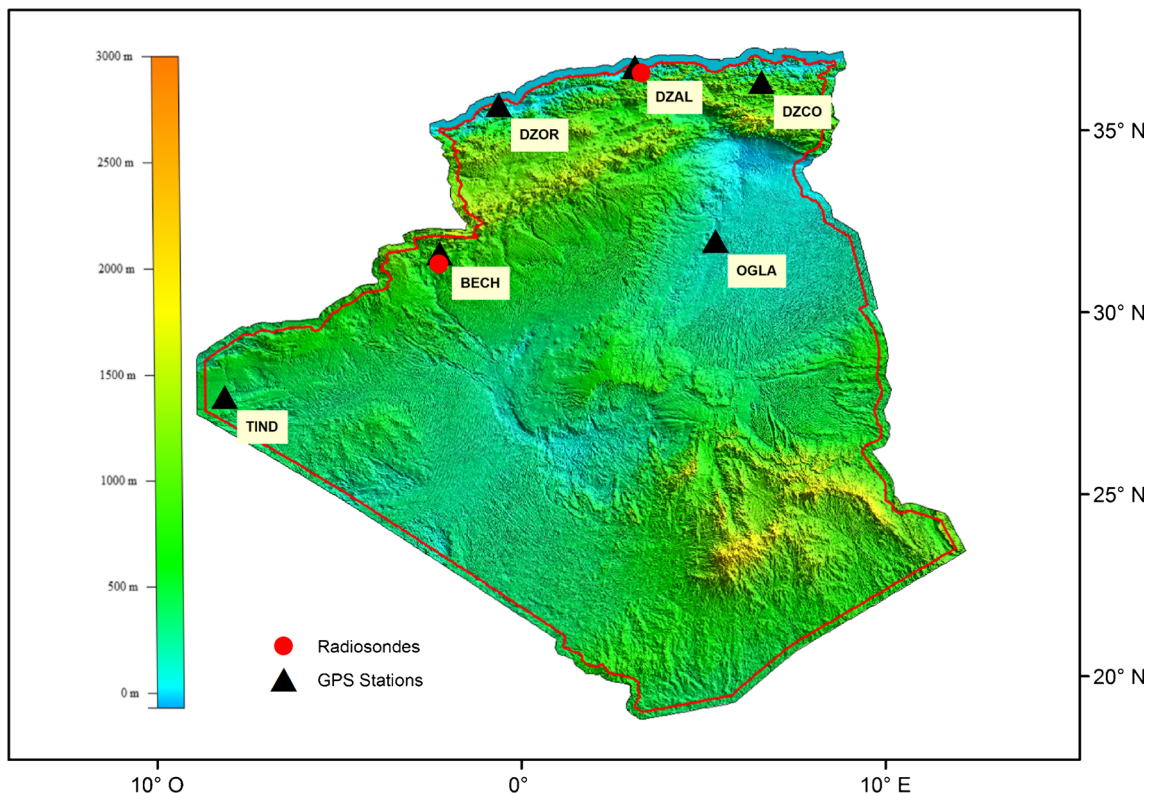


Fig. 3 Map of study area showing the location of GNSS stations (black triangle) and radiosonde sites (red circle) with the surface height gridlines

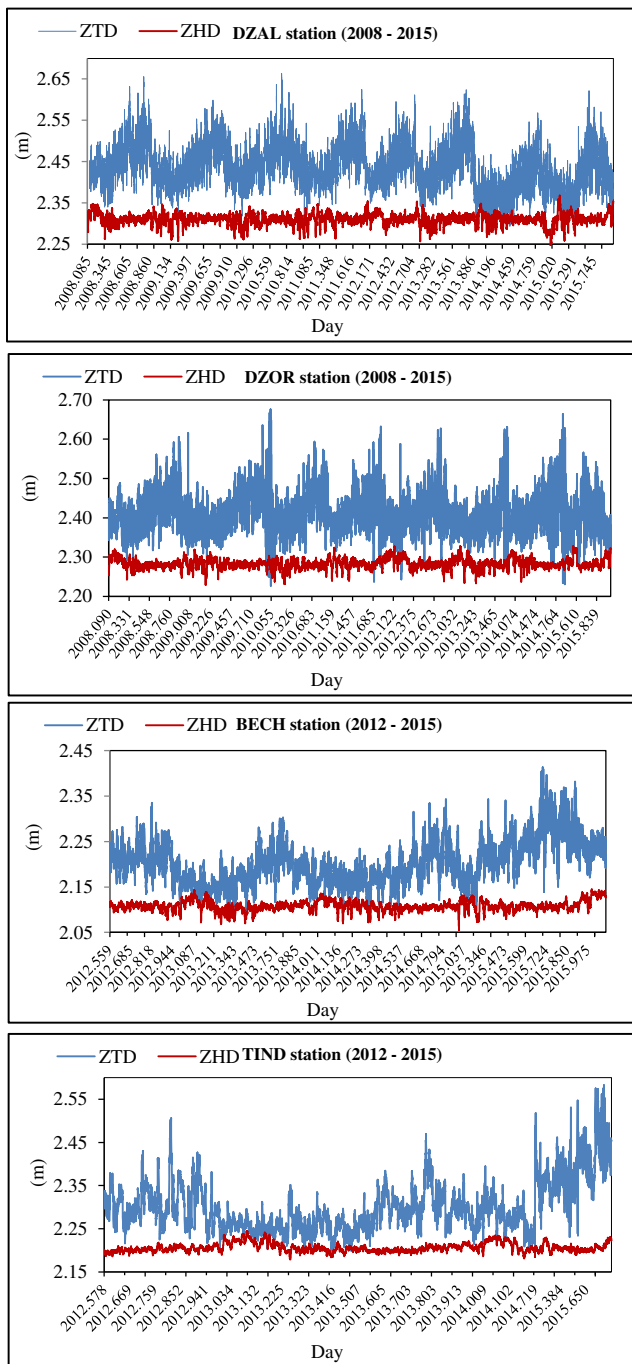


Fig. 4 ZTD and ZHD derived using GPS time series at DZAL, DZOR, BECH, and TIND stations

and ZHD (red curve) time series estimates at DZAL, DZOR, BECH, and TIND stations, calculated using 1-h interval.

The first remark is that the three ZTD curves reveal the existence of a cyclic phenomenon, which is repeated every year. However, the average value of ZTD of the two northern stations DZAL and DZOR is higher than that of the southern stations BECH and TIND.

This difference can be explained by the geographical situation and the change in altitude above the sea for the three stations. Indeed, DZAL and DZOR stations are close to the Mediterranean Sea at an altitude of less 100 m. Therefore, a very high level of humidity is recorded during the warm seasons (May–June–July–August–September) due to the vaporization of sea water; therefore, significant ZTD average amplitude values (2.45 m) are obtained. On the other hand, at BECH and TIND stations, located in the south, respectively at 817 m and 412 m of altitude, characterized by a very hot and dry climate, the ZTD average amplitude values are relatively less important (2.20 m). Furthermore, since the ZTD and ZHD are linearly bound (Formula 1), the values of ZHD follow the same behavior. As shown by Fig. 4, at DZAL and DZOR stations, the ZHD values are stronger in the north with a maximum reaching 2.35 m at DZAL station than in the south, where the maximum value observed at TIND station does not exceed 2.24 m.

All these observations make it possible to confirm that the processing of GPS/GNSS data reveals the presence in the atmosphere of the water vapor index. It remains to quantify them more precisely and compare them with meteorological data recorded by the traditional instruments (radiosonde).

IWV derived from GPS and from ECMWF

For this application, we use GPS and ECMWF IWV data and precipitations recorded during the year of 2014 at four Algerian GPS/GNSS network stations processed by a double difference. This four stations were selected in order to represent the different regions in Algeria, namely the coast with its typical Mediterranean climate in the north (DZAL), the upland (DZCO) which represents a hinge between the Tell and the high plains, and the subtropical desert in the south of the Sahara (BECH, OGLA). A Matlab script was developed for

Table 2 ECMWF IWV model analysis compared to GPS IWV. *N* (number of ECMWF and GPS pairs), STDV (standard deviation), RMS (root mean square), *R* (correlation coefficient), and ΔH (height difference)

Station	<i>N</i>	Bias (kg m ⁻²)	STDV (kg m ⁻²)	RMS (kg m ⁻²)	<i>R</i>	Altitude (m)	EGM96 (m)	ΔH (m)
DZAL	347	4.19	3.61	5.53	0.8574	71.95	25.89	46.06
DZCO	360	-1.56	3.25	3.60	0.8677	591.76	547.58	44.18
BECH	299	-0.23	2.21	2.22	0.9115	863.38	816.68	46.70
OGLA	287	2.05	2.96	3.59	0.8919	174.34	146.54	27.80

Table 3 Coordinates of GPS and radiosonde sites used in this study. The latitudes and longitudes are given in sexagesimal degrees, the height is given with respect to the EGM96 geoid. For the radiosondes, the

distance (dist.) and the height difference (diff. height.) are given compared to the GPS site location

Location	GPS stations				Radiosonde sites					
	Code	Latitude	Longitude	Height (m)	WMO code	Latitude	Longitude	Height (m)	Dist. (km)	Diff. height. (m)
Algiers	DZAL	36° 44' N	03° 06' E	25.89	60,390	36° 40' N	03° 12' E	29.00	9.75	3.11
Bechar	BECH	31° 37' N	02° 14' W	816.68	60,571	31° 30' N	02° 15' W	816.00	7.15	0.68

horizontal and vertical interpolation of the ERA-Interim IWV at the GPS station position.

In this part, we focus on the consistency of GPS IWV and ERA-Interim IWV to estimate the bias between the two dataset for each station as presented in Tables 2 and 3.

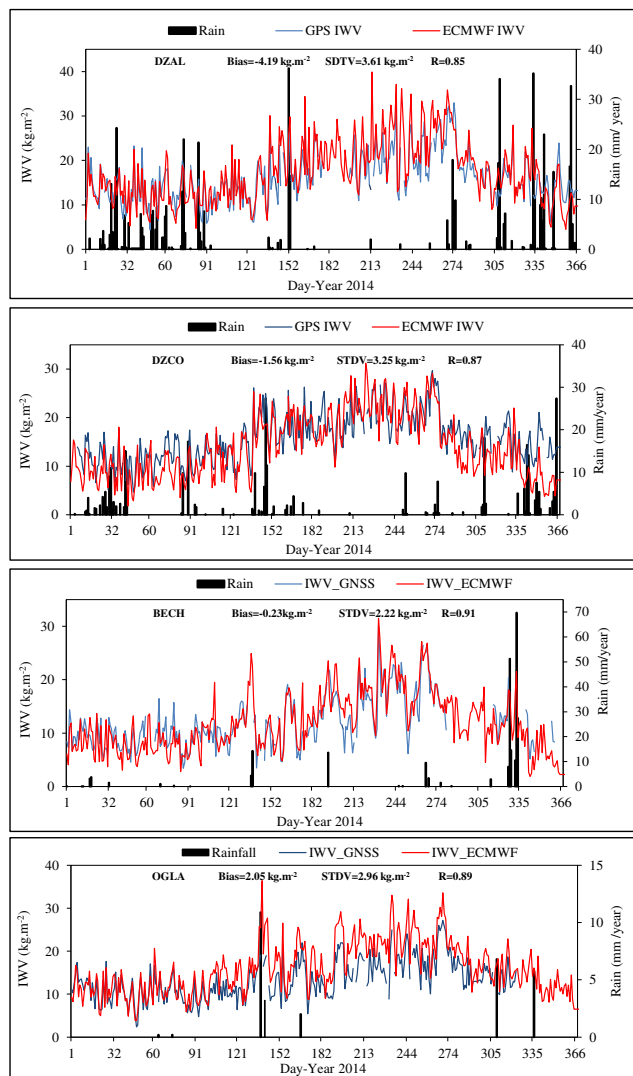


Fig. 5 Time series during year 2014 of IWV derived from GPS (blue lines), ECMWF model (red lines), and rain (black lines) from rain gauge sites nearest GPS stations. At DZAL and DZCO stations (warm Mediterranean climate). At BECH and OGLA stations (warm desert climate)

The four stations DZAL, DZCO, BECH, and OGLA (see Fig. 5 and Table 2) show a high correlation, which exceeds 85% between GPS IWV and ECMWF IWV.

The examination of the IWV values per station leaves the followings remarks: the northern stations (DZAL, DZCO) exhibit larger IWV values than southern stations (BECH, OGLA). This is due mainly to their geographical location and the presence of a significant amount of water evaporation coming from the Mediterranean Sea and they record relatively frequent rains during the autumn and winter seasons.

DZAL station (Algiers) located at a low altitude (25 m), in the vicinity of the Mediterranean Sea with high temperatures in summer, reveals three distinguished periods relating to the average value of IWV during the year: IWV content average around 13 kg m^{-2} for January, February, March, and April, around 22.5 kg m^{-2} for May, June, July, August, and September, and around 16 kg m^{-2} for October, November, and December.

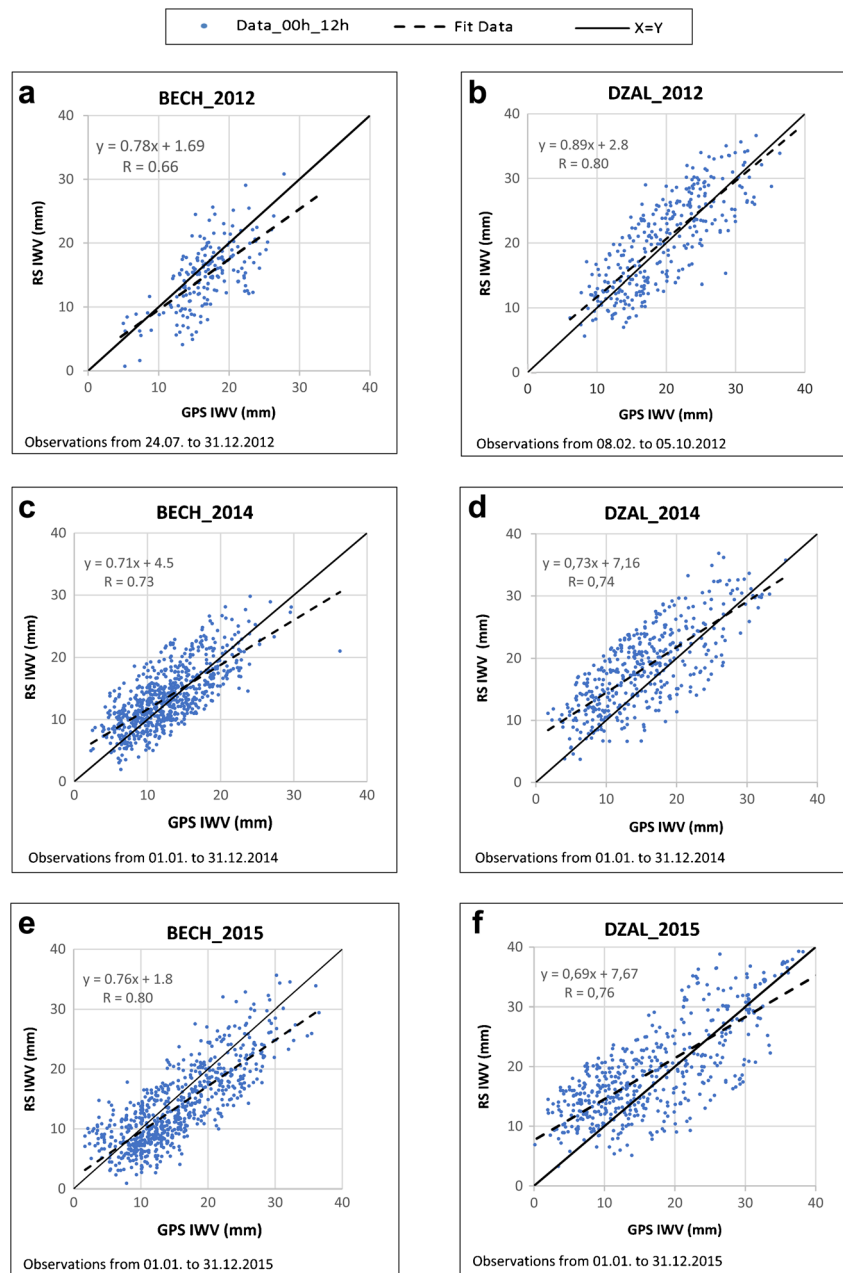
At the same time, DZCO station (Constantine) located at about 70 km from the sea, with an altitude of 550 m and surrounded by forests and dense vegetation, let appear a less important IWV content on yearly average ranges around 10 kg m^{-2} in January, February, March, and April, 20 kg m^{-2} in June, July, August, and September, and 12 kg m^{-2} in October, November, and December.

In the opposite, BECH (Bechar) station located in the south at about 400 km from sea, at altitude 816 m, its IWV content average around 8 kg m^{-2} for January, February, March, April, and May, around 16 kg m^{-2} for June, July, August, September, and October, and around 11 kg m^{-2} for November and December. OGLA (Ouargla) station located also in the south at altitude 144 m, the average of its IWV reached 11.5 kg m^{-2} for January, February, March, April, and May, 20.5 kg m^{-2} for June, July, August, September, and October, and around 15 kg m^{-2} for November and December.

GPS IWV and radiosonde IWV

Figure 6a–f illustrates the comparison of IWV (precipitable water) values in mm obtained after processing the data from two GNSS stations DZAL and BECH and two radiosonde sites of Algiers (WMO code 60390) and BECHAR (WMO

Fig. 6 Comparison of GPS IWV and radiosondes: scatter plots of data of GPS IWV and IWV RS at Bechar (figures on the left) and Algiers (figures on the right). Data 00h_12h (blue point), fit data (discontinuous line), $y = x$ (continuous line)



code 60571). Note that these two stations are located in climatically different regions (see Figs. 1 and 3).

The data used for radiosondes and GPS IWV are those recorded or calculated at 00 h and 12 h.

For Fig. 6a: BECH, it is a station located in the south (hot climate, desert) with 5 months of observations covering part of summer (July–August) known from temperature around 45 °C and a fall period (September–October–November–December) known by significant drop in temperature and thunderstorms. The average value of IWV is 11 mm (11 kg m⁻²). This result is the same as found in the comparison of GPS IWV and ERA-Interim (BECH, Fig. 5).

The correlation remains average ($R = 0.66$) due in large part to the poor quality of GNSS data recorded during this epoch and the short period (5 months) which does not cover the four seasons of the year. For the rest of Fig. 6b–f, the observations are spread over a year or so; the correlation is clearly good with a regression coefficient of about 0.75. The average value of IWV is 16 mm (16 kg m⁻²). This result is the same as found in the comparison of GPS IWV and ERA-Interim (DZAL, Fig. 5).

It is established clearly that the two datasets are concordant and show a good regression with a coefficient R varies between 0.6 and 0.8. We note that the geographical location was

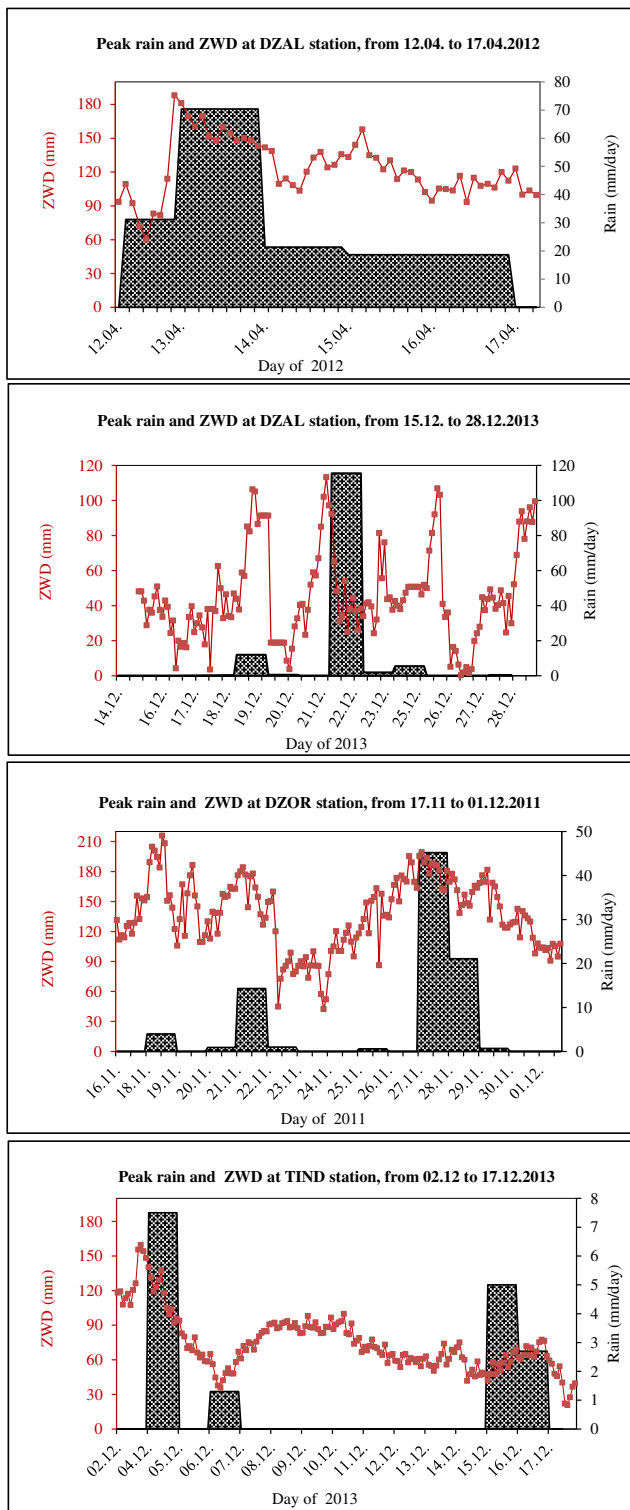


Fig. 7 Rainfall peak and ZWD derived from GPS (red lines) and rainfall peak (black lines). At DZAL station from 12.04 to 17.04.2012 and from 15.12 to 28.12.2013. At DZOR station from 17.11 to 01.12.2011 at 06 h, and at TIND station from 02.12 to 17.12.2013

not highlighted and did not influence the results too much. It has also been noted that the GPS IWV calculation (double difference), the robustness software used, and the support of the different corrections to the values of the radiosondes can improve the results clearly.

GPS IWV and rainfall

After seeing the comparison between the GPS IWV and ECMWF IWV, we now examine the degree of correlation that links them to the precipitation amounts recorded by the National Meteorological Office (NMO).

Figure 5 shows the temporal evolution of IWV (from GPS and from ECMWF) and the rainfall observed during the year 2014 at DZAL, DZCO, BECH, and OGLA stations. At first, for the four stations, we not find real similarity or correlation between precipitations amount and IWV. However, if we examine the behavior of IWV and rain season by season, for the two stations of the north (DZAL, DZCO), the correlation between IWV values and precipitation are clearly established during the first 3 months of the year (January, February, and March). We note that the increase of IWV is regular (around 11 kg m^{-2}) while the rain is abrupt. From April to September, except for a few thunderstorms, the rains are rare and we are witnessing a dry time (springs and summers) and hot due to the dominance of subtropical high pressure systems. During this relatively warm period, evaporation of seawater is important, especially for DZAL (coastal station), resulting in a fairly high humidity and an accumulation of water vapor in the atmosphere. These observations are demonstrated by GPS IWV data and the peak-shaped ECMWF IWV (Fig. 4). Indeed, IWV reaches its maximum around 20 kg m^{-2} . This amount of water vapor will achieve saturation by the end of the summer and will give rise to heavy precipitation in autumn.

For the two south BECH and OGLA stations (subtropical desert), curves of precipitation faithfully reflect the warm desert climate (classification of Köppen BWh) typical of the Sahara characterized by a very long and extremely hot summers and short and very mild winters. The climate is extremely arid and very dry during the year; however, some sporadic precipitations in the form of thunderstorms can occur.

We note that during the periods of January to May and November to December, the increase of IWV is regular (around 9 kg m^{-2}); the rainfall is less and rare. In the period of June to September, on the contrary, the IWV values increase (around 20 kg m^{-2}) without giving significant rainfall.

Comparison of GPS IWV values and some rainfall peaks

In order to better understand the degree of concordance and reliability of the values of the IWV estimated by GPS data, we

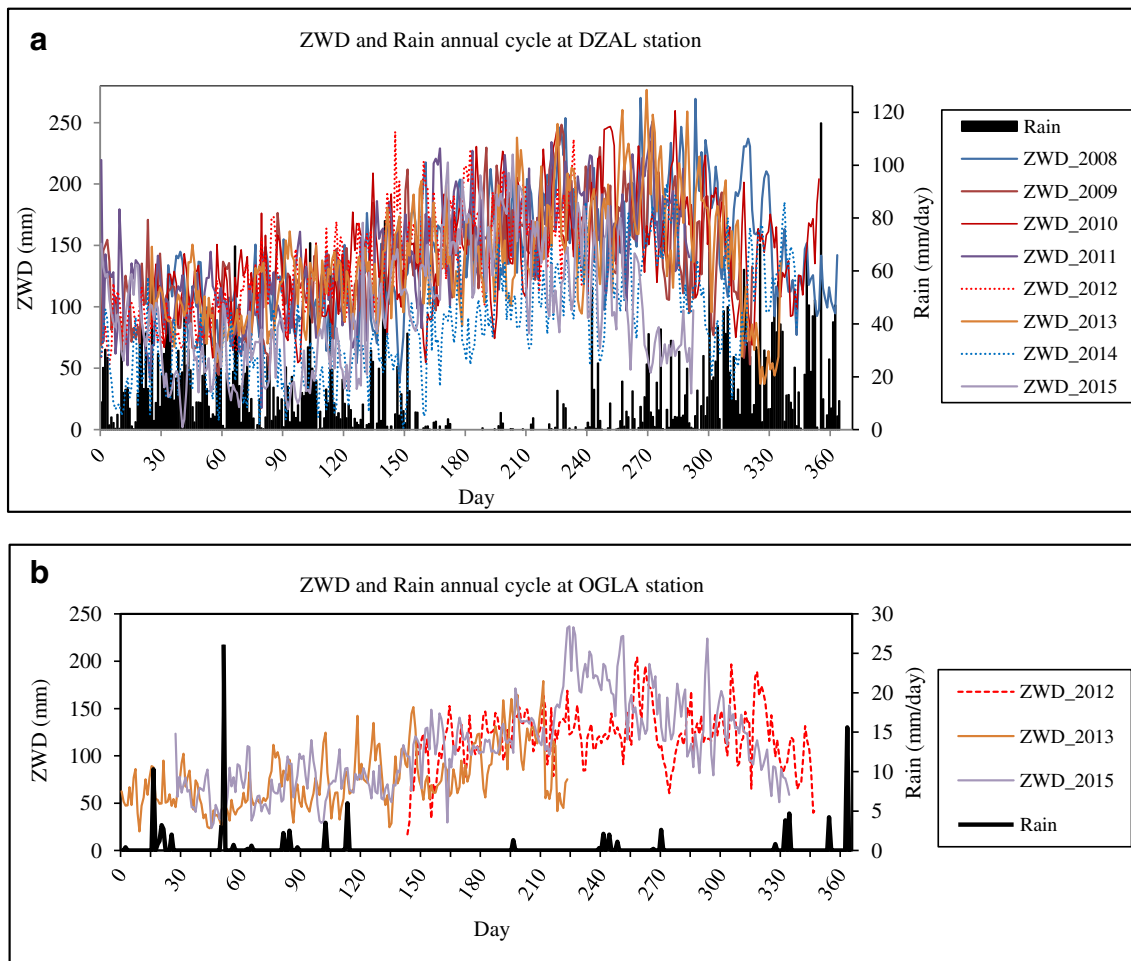


Fig. 8 The time evolution of ZWD estimated by GPS at DZAL northern station and OGLA southern station

examine these values in the vicinity of the few rainfall peaks recorded by the National Meteorological Office.

For example, the meteorological station of Algiers (DZAL) has recorded a peak of 70 mm on 13.04.2012, and 115.5 mm on 21.12.2013, Oran (DZOR) has noted a peak of 14.3 mm on 21.11.2011, 45.2 mm on 27.11.2011, and 21.1 mm on 28.11.2011, while Tindouf (TIND) has registered a peak of 7.5 mm on 04.12.2013 and 5.0 mm on 16.12.2013.

Figure 7 shows hourly variation of ZWD (roughly IWV) values and daily precipitations recorded by the NMO. It is noted that all peaks in precipitations mentioned above are preceded by 2 to 4 h before, by significant values of ZWD estimated by GPS, i.e., a saturation of the atmosphere with water vapor. But at the same time, we noticed that some peaks in ZWD do not necessarily give a precipitation.

The time evolution of ZWD estimated by GPS

To estimate the temporal variation of ZWD (indirectly IWV) and establish if there is a direct relationship with ZWD (IWV) and precipitations, we were interested in the annual cycles of the ZWD, estimated from the GPS data. We used two

geographically and climatically different stations, DZAL station located on the coast, with the data available from 2008 to 2015 and OGLA station in the south, with the available data of 2012, 2013, and 2015. We jointly exploit precipitation data recorded by the ONM during the same periods.

We illustrate in Fig. 8a, b the temporal evolution of GPS estimated ZWD in a northern station and a southern station, near-constant precipitation season (January, February, March, and April).

For the north DZAL station (Figs. 8a) which precipitation season corresponds to the period between days 1 and 150, we observe that the values of the ZWD are constant and relatively low (less than 150 mm). At the arrival of moist air (between days 150 and 270), an abrupt increase of ZWD is observed during a more or less long period. This phase corresponds to a loading of the troposphere into water vapor. Although the troposphere is almost saturated with water, it then reaches a stabilization stage. It is only after about 3 months (between days 150 and 270) that this saturation generates intense and continuous precipitations corresponding to the months of October, November, and December (between days 270 to 365).

At the OGLA Saharan station (Fig. 8b), except for some torrential storms, precipitation is rare not constant and related to the passage of convective mesospheric system ladder. ZWD values are low (less than 100 mm) and the troposphere is not constantly saturated. Between days 230 and 270, ZWD values increase gradually to reach a maximum toward the period of high heat (month of July and August). This difference compared to the DZAL station is due mainly to the difference in stations latitude. The last period (days 270 to 365) corresponds to the gradually decrease of ZWD, with sporadic and relatively low precipitation values.

Conclusion

The Algerian GPS data from six stations are used to estimate locally the IWV and to show its correlation with IWV derived from ECMWF (ERA-Interim model) and radiosondes. The analysis of results obtained shows great correlation between these three datasets and put in evidence the suitability of GPS IWV to estimate the spatial variations of this parameter. The correlation coefficients between GPS IWV and ERA-Interim exceed 85% and the GPS IWV values are slightly important for northern stations (wet and coastal climate) than for the southern ones (dry climate). At the same time, the comparison of GPS IWV and the radiosonde values of two stations belonging to two different climates over 3 years of data show a good similarity with an regression coefficient of around 0.7. The result would have been better if we had GNSS that could also record climatological data to avoid the need for pressure, temperature, and altitude corrections often existing between the GNSS antenna and radiosonde sensor.

In this study, we also noticed the absence of the precipitations despite a high water vapor content recorded from May to August at the four stations (north and south). That is to say, a strong saturation in water vapor in the atmosphere does not give inevitably a precipitation, but the opposite is true; any strong precipitation is the result of a saturation of atmosphere in water vapor.

In our case, the temporal and spatial variations of IWV are well correlated with rains. The local maxima are observed in the precipitation zone, and the maximum IWV is just before the onset of precipitation. The results of this work show that GPS data is an efficient tool and has high spatial and temporal solutions in accordance with the determination of the water vapor content in the atmosphere, a quantity useful for climatology and for numerical weather prediction.

Therefore, continuous GNSS networks established for geodetic, engineering, navigation, etc., can be used for meteorological purposes. However, other areas of shadows require further study and research to provide answers and clarifications, including why the same level of ZWD (roughly IWV) gives only in the same cases intense precipitation? Are there

threshold effects at the spatial and temporal scale that suggest that above an integrated water vapor level precipitation will be triggered?

Acknowledgments We are particularly grateful to our colleagues from geophysical and geodesic laboratories of Luxembourg University especially Addisu H. and Kibrom E. A. We thank the National Meteorological Office for allowing us to use their data. Thanks to the team of the National Institute of Cartography and Remote Sensing, which participated in the installation of the stations and observations campaigns.

References

- Abraha KE, Lewi E, Masson F, Boy JP, Doubre C (2017) Spatial-temporal variations of water vapor content over Ethiopia: a study using GPS observations and the ECMWF model. *GPS Solutions* 21(1):89–99. <https://doi.org/10.1007/s10291-015-0508-7>
- Baltink HK, Van Der Marel H, Van der Hoeven AG (2002) Integrated atmospheric water vapor estimates from a regional GPS network. *J Geophys Res: Atmospheres* 107(D3). <https://doi.org/10.1029/2000JD000094>
- Berrisford P, Dee DPKF, Fielding K, Fuentes M, Kallberg P, Kobayashi S, Uppala S (2009) The ERA-interim archive. ERA report series 1: 1–16
- Bevis M, Businger S, Herring TA, Rocken C, Anthes RA, Ware H (1992) GPS meteorology: remote sensing of atmospheric water vapor using the global positioning system. *J Geophys Res: Atmospheres* 97(D14):15787–15801. <https://doi.org/10.1029/92JD01517>
- Bevis M, Businger S, Chiswell S, Herring TA, Anthes RA, Rocken C, Ware RH (1994) GPS meteorology: mapping zenith wet delays onto precipitable water. *J Appl Meteorol* 33(3):379–386. [https://doi.org/10.1175/15200450\(1994\)033<0379:GMMZWD>2.0.CO;2](https://doi.org/10.1175/15200450(1994)033<0379:GMMZWD>2.0.CO;2)
- Bock O, Doerflinger E (2001) Atmospheric modeling in GPS data analysis for high accuracy positioning. *Physics and Chemistry of the Earth, Part A: Solid Earth and Geodesy* 26(6–8):373–383. [https://doi.org/10.1016/S1464-1895\(01\)00069-2](https://doi.org/10.1016/S1464-1895(01)00069-2)
- Bock O, Guichard F, Janicot S, Lafore JP, Bouin MN, Sultan B (2007a) Multiscale analysis of precipitable water vapor over Africa from GPS data and ECMWF analyses. *Geophys Res Lett* 34:L09705. <https://doi.org/10.1029/2006GL028039>
- Bock O, Bouin M, Walpersdorf A, Lafore JP, Janicot S, Guichard F, Agusti Panareda A (2007b) Comparison of ground based GPS precipitable water vapour to independent observations and NWP model reanalyzes over Africa. *Q.J.R. Meteorol Soc* 133:2011–2027. <https://doi.org/10.1002/qj.185>
- Boehm J, Werl B, Schuh H (2006) Troposphere mapping functions for GPS and very long baseline interferometry from European Centre for Medium-Range Weather Forecasts operational analysis data. *J Geophys Res: Solid Earth* 111(B2). <https://doi.org/10.1029/2005JB003629>
- Böhm J, Niell A, Tregoning P, Schuh H (2006) Global mapping function (GMF): a new empirical mapping function based on numerical weather model data. *Geophys Res Lett* 33(7) <https://doi.org/10.1029/2005GL025546>
- Boutiouta S, Lahcene A (2013) Preliminary study of GNSS meteorology techniques in Algeria. *Int J Remote Sens* 34(14):5105–5118. <https://doi.org/10.1080/01431161.2013.786850>
- Chinowsky P, Schweikert A, Strzepek N, Manahan K, Strzepek K, Schlosser CA (2013) Climate change adaptation advantage for African road infrastructure. *Clim Chang* 117(1–2):345–361. <https://doi.org/10.1007/s10584-012-0536-z>
- Dach R, Hugentobler U, Fridez P, Meindl M (2007) Bernese GPS software version 5.0. Astronomical institute, University of Bern, 640, 114

- Dee DP, Uppala SM, Simmons AJ, Berrisford P, Poli P, Kobayashi S, Bechtold P (2011) The ERA-Interim reanalysis: configuration and performance of the data assimilation system. *Q J R Meteorol Soc* 137(656):553–597. <https://doi.org/10.1002/qj.828>
- Ge M, Gendt G, Rothacher MA, Shi C, Liu J (2008) Resolution of GPS carrier-phase ambiguities in precise point positioning (PPP) with daily observations. *J Geodesy* 82(7):389–399. <https://doi.org/10.1007/s00190-007-0187-4>
- Guerova G (2003) Application of GPS derived water vapor for numerical weather prediction in Switzerland. *PhD thesis*, Institute of Applied Physics, University of Bern, Berne
- Guerova G, Jones J, Dousa J, Dick G, de Haan S, Pottiaux E, Bender M (2016) Review of the state of the art and future prospects of the ground-based GNSS meteorology in Europe. *Atmos Meas Tech* 9(11):5385–5406. <https://doi.org/10.5194/amt-9-5385-2016>
- Hagemann S, Bengtsson L, Gendt G (2003) On the determination of atmospheric water vapor from GPS measurements. *J Geophys Res: Atmospheres* 108(D21). <https://doi.org/10.1029/2002JD003235>
- Haase J, Ge M, Vedel H, Calais E (2003) Accuracy and variability of GPS tropospheric delay measurements of water vapor in the western Mediterranean. *J Appl Meteorol* 42(11):1547–1568
- Heise S, Dick G, Gendt G, Schmidt T, Wickert J (2009) Integrated water vapor from IGS ground-based GPS observations: initial results from a global 5-min dataset. *Ann Geophys* 27(7):2851–2859. <https://doi.org/10.5194/angeo-27-2851-2009>
- Jones J (2010) An assessment of the quality of GPS water vapor estimates and their use in operational meteorology and climate monitoring. *PhD thesis*, University of Nottingham. http://eprints.nottingham.ac.uk/11287/1/JJ_Thesis_Final.pdf
- Li Z, Muller JP, Cross P (2003) Comparison of precipitable water vapor derived from radiosonde, GPS, and moderate-resolution imaging spectroradiometer measurements. *J Geophys Res* 108(D20):4651. <https://doi.org/10.1029/2003JD003372>
- Namaoui H, Kahlouche S, Belbachir AH, Van Malderen R, Brenot H, Pottiaux E (2017) GPS water vapor and its comparison with radiosonde and ERA-Interim data in Algeria. *Adv Atmos Sci* 34(5):623–634. <https://doi.org/10.1007/s00376-016-6111-1>
- Rocken C, Ware RH, Hove TV, Solheim F, Alber C, Johnson J, Bevis M, Businger S (1993) Sensing atmospheric water vapor with the global positioning system. *Geophys Res Lett* 20:2631–2634
- Roeckner E, Bäuml G, Bonaventura L, Brokopf R, Esch M, Giorgetta M, Rhodin A (2003) The atmospheric general circulation model ECHAM 5. PART I: model description. Report/MPI für Meteorologie, 349. http://pubman.mpdl.mpg.de/pubman/item/escidoc:995269/component/escidoc:995268/max_scrip_p_349.pdf
- Vey S, Dietrich R., Fritsche M, Rulke A, Steigenberger P, Rothacher M (2009) On the homogeneity and interpretation of precipitable water time series derived from global GPS observations. *J Geophys Res (D: Atmos)*, 114. <https://doi.org/10.1029/2008JD010415>
- Wang J, Zhang L (2009) Climate applications of a global, 2-hourly atmospheric precipitable water dataset derived from IGS tropospheric products. *J Geodesy* 83(3):209–217. <https://doi.org/10.1007/s00190-008-0238-5>
- Wolfe DE, Gutman SI (2000) Developing an operational, surface-based, GPS, water vapor observing system for NOAA: network design and results. *J Atmos Ocean Technol* 17:426–440